Published in final edited form as:
Magn Reson Med. 2008 March ; 59(3): 515–520. doi:10.1002/mrm.21526.

Magnetic Microparticle Aggregation For Viscosity Determination By Magnetic Resonance

Rui Hong[†], **Michael J. Cima**[‡], **Ralph Weissleder**[†], and **Lee Josephson**[†,*]

[†]Center for Molecular Imaging Research, Harvard Medical School, Massachusetts General Hospital, 149 13th street, Charlestown, MA 02129

[‡]Department of Material Science and Engineering, Massachusetts Institute of Technology, Room 12-011, 77 Massachusetts Avenue, Cambridge, MA 02139

Abstract

Micron-sized magnetic particles were induced to aggregate when placed in homogeneous magnetic fields, like those of magnetic resonance (MR) imagers and relaxometers, and then spontaneously returned to their dispersed state when removed from the field. Associated with the aggregation and dispersion of the magnetic particles were time dependent increases and decreases in the spin-spin relaxation time (T_2) of the water. Magnetic nanoparticles, with far smaller magnetic moments per particle, did not undergo magnetically induced aggregation, and exhibited time independent values of T_2. The rate of T_2 change associated with magnetic micro-particle aggregation was used to determine the viscosity of liquid samples, providing a method that can be of particular advantage for determining the viscosity of small volumes of potentially biohazardous samples of blood or blood plasma.

Keywords

magnetic particle; nanoparticle; aggregation; relaxivity; viscosity

Introduction

Magnetic nanoparticles (~10–100 nm) and magnetic microparticles (>100 nm serve as important classes of materials for use as MR contrast agents and in cell sorting applications. Polysaccharide coated magnetic nanoparticles (NPs), like the MION-47 used in the current study, are used as intravenously administered magnetic resonance imaging (MRI) contrast agents due to their high relaxivities, low toxicity and ready degradation in vivo. Due to their successful development as clinically useful MR contrast agents, NP effects on water relaxation have often been described (1–8). Larger polystyrene based micron-sized magnetic particles (MPs) lack the biodegradability of NPs and have been used as gastrointestinal contrast agents where elimination of the intact MP prevents absorption and toxicity (9–11). MPs are widely used for applications requiring magnetic manipulation, such as immunoassays or cell sorting, since NPs cannot be manipulated by hand held magnets and without the assistance of magnetic grids (12,13). Though NPs and MPs are available from many commercial sources, these two types of materials are currently used principally in different applications, and there has been little motivation to compare their effects on water relaxation rates. However, the realization that the aggregation of magnetic NPs (and potentially MPs) can be sensed by MR, and used to assay molecular targets in vitro (14–16), or as components of implantable and removable

Corresponding author: Lee Josephson, Email address: josephso@helix.mgh.harvard.edu.

sensors (17), provides a motivation for understanding the effects of diverse types of materials on water relaxation, since toxicity and biodegradability have minimal relevance for these applications. In comparing the effects of the MION-47 NP and the MP (Dynal MyOne beads) on water relaxation, we noted a pronounced time dependence of the latter material in magnetic fields.

When placed in a homogenous magnetic field, solutions of non-settling, micron-sized superparamagnetic MPs like the MyOne underwent time dependent increases in the water proton spin-spin relaxation time, T_2, due to magnetic field induced MP aggregation. This observation endows MPs certain advantages over NPs in sensor applications, which will be reported on in due course. Here we describe the features of the magnetic field induced MP aggregation and the associated water proton T_2 increase, and show how this aggregation provides a magnetic resonance based method for determining media viscosity.

Although a variety of techniques are used to measure viscosity, conventional capillary, falling body and rotational viscometers have shortcomings when used to determine the viscosity of small volumes of blood or blood plasma, see below. Yet in the medical arena patients with multiple myeloma or Waldenström's macroglobulinemia suffer from lethargy, bleeding, headaches, vision problems and numbness due to abnormal elevations of blood viscosity correctable by apheresis (18). The viscosity of whole blood or plasma (blood minus cells) is also of significant interest in diverse conditions ranging from thrombogenic diseases and microcirculatory disorders to sickle cell anemia (19–22). An MP based magnetic resonance method of determining viscosity, with dedicated MR instrumentation designed for this purpose, might be a preferred method for determining the viscosity of small biohazardous samples such as those found in a clinical chemistry setting.

Methods

The MyOne-COOH magnetic microparticle, denoted as MP, was purchased from Invitrogen (Carlsbad, CA). The magnetic nanoparticle, denoted as NP, was the dextran coated MION-47 made as described (23). All the other chemicals and solvents were purchased from Aldrich (St. Louis, MO). The value of 8000 Fe per NP was used (24). The value of 2.8×10^9 Fe atoms per MP was determined from the manufacturer's number of particles per mL and the iron concentration. Particle settling was the percent change in the optical density at 405 nm at room temperature for 2 hours. All experiments were performed in phosphate buffered saline (PBS), pH 7.4, unless otherwise noted.

Particle sizes were measured on a Zetasizer 1000HS light scattering instrument (Malvern Instruments, Southborough, MA). Relaxation times were measured on a relaxometer at 40 °C, 0.47 T and 20 MHz (Minispec mq20, Bruker, Billerica, MA). T_2 was measured using a 200 data point spin-echo CPMG pulse sequence with a pulse separation of 0.5 ms and 8 scans. T_1 was measured using a 12 data point inversion-recovery pulse sequence with pulse separations ranging from 5 to 1000 ms and 4 scans.

Magnetic moments (at 25 °C) were obtained on a superconducting quantum interference device (SQUID) magnetometer (Quantum Design, San Diego, CA). Phase contrast micrographs of MPs exposed to a magnetic field were obtained by diluting microparticles in unsolidified 0.5% agarose, and subjecting them to the magnetic field of the relaxometer in which the agar solidified. Agar was sectioned and observed with a Nikon Eclipse E400 microscope (Nikon Instruments Inc., Melville, NY). Viscosity was measured by using a cross-arm viscometer (Cole-Parmer, Vernon Hills, IL), and expressed in unit of centistokes (cSt). To obtain MR images at 4.7 T (Bruker, Billerica, MA), 80 μL samples were placed in a section of a 384 well plate and CPMG spin echo images obtained at room temperature (TR= 2000 msec, TE = 40,

80, 120, 160 msec, FOV = 4 cm, 256 × 256 matrix, slice thickness = 1.5 mm). Images were converted to T_2 maps as described (25).

Results

The physical characteristics of the magnetic microparticle (MP), and magnetic nanoparticle (NP) are summarized in Table 1. The MP is a microsphere comprised of polystyrene with superparamagnetic iron oxide crystals entrapped within its matrix. A more detailed characterization of the MyOne beads (MPs) has shown that 7–8 nm iron oxide nanoparticles embedded in the polymer matrix are responsible for the magnetic properties of the beads (26). The NP was a monodisperse crystal of superparamagnetic iron stabilized by a thick (10 nm) coating of T-10 dextran. The MP and NP were quite different in size, 1000 nm and 30 nm in diameter respectively, though they shared the property of remaining suspended for extended periods of time in a gravitational field. The NP remained suspended due to Brownian motion or steric repulsion of the coating, since it is quite dense. (Both components of the NP, iron oxide and dextran, have densities greater than water. Iron oxide density = 5–6 g/cm^3; dextran density = 1.17 g/cm^3). The larger MP remained suspended presumably because its buoyant density was close to that of the media (Polystyrene density varies with the type but is between 1.0 and 1.1 g/cm^3). The MP and NP had similar magnetic moments per gram of iron and similar R_2 relaxivities per mole of iron ($s^{-1}mM^{-1}$) as shown in Table 1. The NP had an R_1 of 18 $s^{-1}mM^{-1}$, indicating that a high accessibility of water to the surface of the iron oxide, while the MP had an R_1 of less than 1 $s^{-1}mM^{-1}$, indicating that the surface of the iron oxide crystals was shielded from water by a matrix of polymer. Another difference between the MP and the NP was apparent when relaxivities or magnetic moments were calculated on per particle basis. The MP had 2.8×10^9 Fe atoms per MP compared to 8000 Fe for the NP, or 350,000 times more iron. Hence on per particle rather than per iron basis, the R_2 and magnetic moment of the MP were far greater than those of the NP. For example, the magnetic moment of a single MP was about 4×10^5 times larger than that of a single NP.

The spin-spin relaxation times (T_2s) of the MP and NP solutions as a function of time were measured and the results are shown in Figure 1. Aqueous solutions of MPs or NPs were placed within either 5 or 10 mm NMR tubes and incubated at 40 °C prior to the T_2 measurements, which were obtained at 0.47 T and 40 °C. In the 0.47 T field of relaxometer, the T_2 of the MP solution increased from ~130 ms to ~400 ms in less than 6 minutes, and leveled off by 10–15 minutes (data not shown). After 8 minutes, the tube was removed from the relaxometer and incubated for 2 minutes at 40 °C in a water bath without agitation and in the absence of an additional magnetic field. Withdrawal from the magnetic field produced a drop in T_2 to about the original value of 130 ms, which again increased when placed in the relaxometer. Thus solutions of MPs showed increasing T_2 values in the relaxometer, an increase that was readily reversed with short incubation outside the magnetic field. On the other hand, solutions of NPs had completely time independent values of T_2 in the relaxometer. In fact NP solutions had constant T_2 not only for 30 minutes (Figure 1), but for up to 24 hours (data not shown). Thus, solutions of MPs and NPs behaved differently in the relaxometer, with MP solution undergoing T_2 increases, which were readily reversed by removing the sample from the magnetic field, while solutions of NPs gave time independent T_2 values.

To determine if placing MPs in the 0.47 T magnetic field altered their physical state, i.e. aggregated or dispersed, solutions of MPs were diluted into a molten agar solution (0.5 % w/v in water) and allowed to gel either in the magnetic field at 40 °C or in a water bath at 40 °C. After sectioning the solidified agar, the distribution of MPs was examined by microscopy (Figure 2). When gelation occurred in the magnetic field, MPs existed as large aggregates, with large volumes of solution completely devoid of MPs (Figure 2A). In contrast, when agar

gelation occurred in the water bath, MPs existed as dispersed, evenly distributed one micron microspheres (Figure 2B).

To determine if the MP aggregation and the time dependent T_2 increase reflected design of the relaxometer magnet or peculiarities of the sample tube, we examined the time dependent behavior of NPs and MPs in the 4.7 T magnet of an MR imager. Solutions of MPs and NPs were placed in the wells of a 384-well microtiter plate and the T_2 weighted images were obtained at 10-minute intervals. As shown in Figure 3A, a time dependent T_2 increase was again observed for the MP solution in this magnet field. In addition, after 60 minutes the T_2 of the MP solution in PBS became markedly heterogeneous, as would be expected given the development of large volumes of solution void of MPs seen with Figure 2B. Since the formation MP aggregates required MP movement, we reasoned that increasing media viscosity should retard the T_2 increase. As shown in Figure 3A, when the viscosity of MPs in PBS was increased to 8.9 cSt by the addition of Triton X-100, the time dependent increase in T_2 was suppressed. In contrast, the T_2 of the NP solution was time independent even in PBS. The time dependent increase of the average T_2s of wells shown in Figure 3A was further investigated and the results are shown in Figure 3B. The MP solution showed a time dependent T_2 increase progressively over 60 minutes, an increase that was dramatically slowed by increased viscosity. On the other hand, the T_2 of the NP solution was time independent. These results are consistent with the particle clustering observed at 0.47 T (Minispec), thus suggesting the generality of the magnetic field induction in different fields. The difference between the T_2 values recorded in the Minispec and the imager is due to a combined effect of temperature (room temperature versus 40 °C), and the magnetic field dependence of T_2 (7).

Since the magnetic field induced MP aggregation was slowed by an increase in medium viscosity (Figure 3B), we examined whether T_2 changes might be used as a method to assay the viscosity of serum. Synthetic “myeloma sera” were created by the addition of bovine IgG to fetal bovine serum, to approximate the composition of myeloma sera. Time dependent T_2 changes of an MP suspension in the sera were determined in the relaxometer. As shown in Figure 4A, the change in T_2 was linear with time, with the rate of T_2 change decreasing as the serum viscosity increased. Importantly, a linear relationship was found between the rate of T_2 change (in Figure 4A) and the inverse of solution viscosity (η) as shown in Figure 4B. The observation of a linear relationship between the rate of change in T_2 and the reciprocal of the solution viscosity suggests that these effects could be used to measure the unknown viscosities of other solutions. Since our method of viscosity determination relies on the rate of T_2 increase (Figure 4), it can be performed on solutions with a wide range of intrinsic T_2 values. We note that our method of measuring viscosity is a relative one and that to obtain absolute viscosity values, a calibration standard must be employed.

The linear relationship between the rate of change in T_2 and the reciprocal of the solution viscosity (Figure 4) can be obtained through an examination of the behavior of colloidal aggregation. The particle coagulation rate (r_o) for the rapid coagulation regime (all collisions resulting in aggregation) is described by:

$$r_o = 8\pi D_p a c_0^2 \quad [1]$$

where is the particle diffusivity, is the particle radius, and is the initial particle concentration. According to the Stokes-Einstein relation, the particle diffusivity is given by

$$D_p = \frac{kT}{6\pi a \eta} \quad [2]$$

where is the Boltzmann constant, is the temperature, and is the viscosity. Roch, *et al.* (5) have shown that, in the large sphere limit, the solvent water proton T_2 increases during particle aggregation, such that

$$T_2 \propto \tau_D \quad [3]$$

where τ_D $(=R_a^2/D_w)$ is the time required for water translational diffusion around a particle or an aggregate; R_a is the radius of the agglomerate, which is proportional to r_0 in equation 1, and D_w is the diffusivity of water. Shapiro, *et al*. (6) discussed the fact that the agglomerates are not densely packed but behave as fractal agglomerates, so that the relationship between agglomerate size and number of particles within the agglomerate is given by

$$R_a = n^{1/df} \quad [4]$$

where n is the number of particles in an agglomerate and is the fractal dimension, which has values between 1.75 and 2.3. Thus, a combination of equation 3 and equation 4 suggests that the T_2 of water is linearly related to the number of particles within the aggregate if the fractal dimension is approximately 2. Furthermore, an examination of equation 1 and equation 2 shows that the rate of change of the number of particles in an agglomerate will be inversely proportional to the viscosity of the medium. Thus, we expect the rate of T_2 change to be inversely proportional to the viscosity, and this is consistent with the results shown in Figure 4.

Discussion

Micrographs of the high and low T_2 states (Figure 2), and the effects of viscosity on retarding T_2 changes (Figure 3 and Figure 4), lead to the model of magnetic field induced MP aggregation shown in Figure 5. In the absence of an applied magnetic field (Figure 5A), MPs have no magnetic remanence due to the superparamagnetic nature of the iron oxide. With the application of a homogeneous magnetic field, the MPs become magnetic and their magnetic moments align with the applied magnetic field (Figure 5B). When MPs move into close proximity by diffusion, aggregation occurs because magnetic coupling (magnetic attraction between MPs) results (Figure 5C). With the removal of the MP aggregates from a magnetic field, the Neel relaxation of superparamagnetic iron oxide crystals eliminates magnetic coupling, and thermal fluctuations return MPs to a dispersed state (Figure 5D). The magnetizations of superparamagnetic materials saturate at 0.47 T (27,28) so that if our particles are saturated at 0.47 T, they will certainly remain saturated at the higher flux density of 4.7 T.

The model is supported by estimates of the ratio, λ, of the magnetic dipolar energies of the particles to the energy available from the environment to cause random, thermal reorientation of the particles (29). Here, $\lambda = \mu_0\mu^2/(4\pi k_B T d^3)$, where μ_0 is the permeability of vacuum, μ the magnetic moment of one particle, and d the diameter of the particle. For values of λ greater than 2, magnetic coupling is typically strong enough to overcome thermal motion. From the magnetic moments obtained (Table 1), λ of the MP is about 1.8×10^4 compared to that of the NP which is 3.6×10^{-3}. Thus the MP aggregation and the increasing T_2s of MPs exhibited in homogeneous magnetic fields were due to the large magnetic moment per particle, which lead to stabilized MP aggregation, while the smaller magnetic moment of NPs yielded magnetic coupling not strong enough to overcome thermal randomization or permit aggregate formation.

It should be noted that the magnetic field induced aggregation of MPs described here results in increases in the water T_2, while the previously described ligand clustering of NPs results in

T_2 decreases (14,16). There are two non-exclusive explanations of these different effects on T_2. The first proposes that MP aggregation leads to heterogeneous concentrations of MPs in different volumes of solution. Supporting this view were the discrete volumes of solution free of aggregate seen by microscopy (Figure 2) and the development of heterogeneous solution T_2s when the MP solutions were placed in a 4.7 T magnetic field for 60 minutes (upper right image of Figure 3A). A second explanation for the differing effects of NPs and MPs on T_2 of the solvent comes from the outer sphere diffusion theory. This theory employs two parameters, τ_d, the diffusion time for water, and $\Delta\omega$, the difference in angular frequency between the local field experienced by a proton at the equatorial line of the particle or cluster surface and in the bulk, to describe the effect of the size of magnetic spheres on T_2 (1–6). Outer sphere diffusion theory predicts that the T_2 of the water will decrease as NP size increases (or NP aggregates form), since the motional averaging condition ($\Delta\omega\tau_d < 1$) is fulfilled. However, for micron-sized MPs (or MP aggregates), T_2 will increase with increasing particle size, since the motional average condition is not fulfilled ($\Delta\omega\tau_d > 1$). Thus outer sphere relaxation theory provides a second explanation for the increase in T_2 seen with MP aggregation.

The MP based magnetic resonance method of viscosity determination might be a preferred method over conventional methods of viscosity measurement in the clinical laboratory where a small sample size and the containment of biohazards are considerations. For our relaxometry measurements, a sample of 400 μL was used, though samples as small as 50 μL have been used without loss of accuracy or precision (Taktak and Josephson, unpublished data). Further reductions of sample size seem quite feasible based on successful efforts to develop micro MR devices (30–32). In contrast, falling body, rotational, and capillary viscometers require a minimum of 2 mL, while the Ostwald viscometer requires 5 mL (21). The use of disposable glassware and MPs could be a second significant advantage of the MR based method of viscosity determination in the clinical laboratory, where measurements are made on biohazardous samples. Although we used NMR tubes (Norell) for the current study, an examination of other glassware and plastic ware indicated many gave water T_2 values of coefficient of variation (CV) less than 2 % in the relaxometer used. (CV is defined as a standard deviation of T_2 divided by a mean of T_2)

Although we employed a conventional laboratory 0.47 T relaxometer and 4.7 T MR imager to measure T_2, in the future the determination of viscosity by T_2 might employ simpler and cheaper instrumentation designed for this purpose. Recent advances in MR instrumentation might be applied to the design of such an instrument and include single sided profilers (33), portable high-resolution NMR spectroscopes (34) and portable micro NMR instruments (35, 36). A simple, portable relaxometer has been described by one commercial entity (37).

Our study of the magnetic field induced MPs aggregation and associated T_2 changes can influence further development in three areas. As noted, the method is well suited for assessing the viscosity of biohazardous fluids, and may lead to an increased appreciation of this key physical property in normal and disease states. Second, by using MPs which disperse in organic solvents, e.g. MPs with a hydrophobic surface rather than the hydrophilic surfaces of the current MP, the method might be adapted to measuring the viscosity of organic solvent based polymer solutions used in many industrial applications. Finally, understanding how MPs respond to homogeneous magnetic fields, and how that response affects proton relaxation times, is essential to the use of MPs in NMR based particle agglutination assays for biomolecular targets. With their larger magnetic moment and higher R_2 per particle (Table 1), the replacement of NPs by MPs may lead to faster or more sensitive MR based assays.

Acknowledgements

We thank Fred Reynolds (CMIR) for help on viscosity measurement and valuable discussions. This work was supported by National Institutes of Health grants R01-EB004626 and R01-EB00662.

References

1. Muller RN, Gillis P, Moiny F, Roch A. Transverse relaxivity of particulate MRI contrast media: from theories to experiments. Magn Reson Med 1991;22:178–182. [PubMed: 1812343]
2. Gillis P, Koenig SH. Transverse relaxation of solvent protons induced by magnetized spheres: application to ferritin, erythrocytes, and magnetite. Magn Reson Med 1987;5:323–345. [PubMed: 2824967]
3. Brooks RA, Moiny F, Gillis P. On T2-shortening by weakly magnetized particles: the chemical exchange model. Magn Reson Med 2001;45:1014–1020. [PubMed: 11378879]
4. Yung KT. Empirical models of transverse relaxation for spherical magnetic perturbers. Magn Reson Imaging 2003;21:451–463. [PubMed: 12878254]
5. Roch A, Gossuin Y, Muller RN, Gillis P. Superparamagnetic colloid suspensions: Water magnetic relaxation and clustering. J Magn Magn Mater 2005;293:532–539.
6. Shapiro MG, Atanasijevic T, Faas H, Westmeyer GG, Jasanoff A. Dynamic imaging with MRI contrast agents: quantitative considerations. Magn Reson Imaging 2006;24:449–462. [PubMed: 16677952]
7. Bulte JWM, Brooks RA, Moskowitz BM, Bryant LH, Frank JA. Relaxometry and magnetometry of the MR contrast agent MION-46L. Magn Reson Med 1999;42:379–384. [PubMed: 10440963]
8. Majumdar S, Zoghbi S, Pope CF, Gore JC. A quantitative study of relaxation rate enhancement produced by iron oxide particles in polyacrylamide gels and tissue. Magn Reson Med 1989;9:185–202. [PubMed: 2716504]
9. Ericsson A, Lonnemark M, Hemmingsson A, Bach-Gansmo T. Effect of superparamagnetic particles in agarose gels. A magnetic resonance imaging study. Acta Radiol 1991;32:74–78. [PubMed: 2012737]
10. Niemi P, Katevuo K, Kormano M, Baksaas I, Bach-Gansmo T, Maenpaa J. Superparamagnetic particles as gastrointestinal contrast agent in magnetic resonance imaging of lower abdomen. Acta Radiol 1990;31:409–411. [PubMed: 2206698]
11. Lonnemark M, Hemmingsson A, Carlsten J, Ericsson A, Holtz E, Klaveness J. Superparamagnetic particles as an MRI contrast agent for the gastrointestinal tract. Acta Radiol 1988;29:599–602. [PubMed: 3166884]
12. Whitesides GM, Kazlauskas RJ, Josephson L. Magnetic separations in biology. Trends Biotechnol 1983;1:144–148.
13. Franzreb M, Siemann-Herzberg M, Hobley TJ, Thomas OR. Protein purification using magnetic adsorbent particles. Appl Microbiol Biotechnol 2006;70:505–516. [PubMed: 16496138]
14. Josephson L, Perez JM, Weissleder R. Magnetic nanosensors for the detection of oligonucleotide sequences. Angew Chem Int Edit 2001;40:3204–3208.
15. Perez JM, Josephson L, Weissleder R. Use of magnetic nanoparticles as nanosensors to probe for molecular interactions. Chembiochem 2004;5:261–264. [PubMed: 14997516]
16. Perez JM, Josephson L, O'Loughlin T, Hogemann D, Weissleder R. Magnetic relaxation switches capable of sensing molecular interactions. Nat Biotechnol 2002;20:816–820. [PubMed: 12134166]
17. Sun EY, Weissleder R, Josephson L. Continuous analyte sensing with magnetic nanoswitches. Small 2006;2:1144–1147. [PubMed: 17193579]
18. Zarkovic M, Kwaan HC. Correction of hyperviscosity by apheresis. Semin Thromb Hemost 2003;29:535–542. [PubMed: 14631553]
19. Lipowsky HH. Microvascular rheology and hemodynamics. Microcirculation 2005;12:5–15. [PubMed: 15804970]
20. Stuart J, Nash GB. Technological advances in blood rheology. Crit Rev Clin Lab Sci 1990;28:61–93. [PubMed: 2121160]
21. Rosencranz R, Bogen SA. Clinical laboratory measurement of serum, plasma, and blood viscosity. Am J Clin Pathol 2006;125:S78–S86. [PubMed: 16830959]

22. Somer T, Meiselman HJ. Disorders of blood viscosity. Ann Med 1993;25:31–39. [PubMed: 8435185]
23. Josephson L, Tung CH, Moore A, Weissleder R. High-efficiency intracellular magnetic labeling with novel superparamagnetic-tat peptide conjugates. Bioconjug Chem 1999;10:186–191. [PubMed: 10077466]
24. Reynolds F, O'Loughlin T, Weissleder R, Josephson L. Method of determining nanoparticle core weight. Anal Chem 2005;77:814–817. [PubMed: 15679348]
25. Hogemann D, Ntziachristos V, Josephson L, Weissleder R. High throughput magnetic resonance imaging for evaluating targeted nanoparticle probes. Bioconjug Chem 2002;13:116–121. [PubMed: 11792186]
26. Fonnum G, Johanson C, Molteberg A, Morup S, Aksenes E. Characterization of Dynabeads by magnetization measurements and Mossbauer spectroscopy. J Magn Magn Mater 2005;293:41–47.
27. Josephson L, Lewis J, Jacobs P, Hahn PF, Stark DD. The effects of iron oxides on proton relaxivity. Magn Reson Imaging 1988;6:647–653. [PubMed: 2850434]
28. Jung CW, Jacobs P. Physical and chemical properties of superparamagnetic iron oxide MR contrast agents: ferumoxides, ferumoxtran, ferumoxsil. Magn Reson Imaging 1995;13:661–674. [PubMed: 8569441]
29. Klokkenburg M, Vonk C, Claesson EM, Meeldijk JD, Erne BH, Philipse AP. Direct imaging of zero-field dipolar structures in colloidal dispersions of synthetic magnetite. J Am Chem Soc 2004;126:16706–16707. [PubMed: 15612692]
30. Wolters AM, Jayawickrama DA, Sweedler JV. Microscale NMR. Curr Opin Chem Biol 2002;6:711–716. [PubMed: 12413558]
31. Olson DL, Lacey ME, Webb AG, Sweedler JV. Nanoliter-volume 1H NMR detection using periodic stopped-flow capillary electrophoresis. Anal Chem 1999;71:3070–3076. [PubMed: 10450155]
32. Olson DL, Norcross JA, O'Neil-Johnson M, Molitor PF, Detlefsen DJ, Wilson AG, Peck TL. Microflow NMR: concepts and capabilities. Anal Chem 2004;76:2966–2974. [PubMed: 15144211]
33. Manz B, Coy A, Dykstra R, Eccles CD, Hunter MW, Parkinson BJ, Callaghan PT. A mobile one-sided NMR sensor with a homogeneous magnetic field: the NMR-MOLE. J Magn Reson 2006;183:25–31. [PubMed: 16891134]
34. Perlo J, Demas V, Casanova F, Meriles CA, Reimer J, Pines A, Blumich B. High-resolution NMR spectroscopy with a portable single-sided sensor. Science 2005;308:1279. [PubMed: 15817815]
35. Sillerud LO, McDowell AF, Adolphi NL, Serda RE, Adams DP, Vasile MJ, Alam TM. 1H NMR Detection of superparamagnetic nanoparticles at 1T using a microcoil and novel tuning circuit. J Magn Reson 2006;181:181–190. [PubMed: 16698297]
36. Halse ME, Coy A, Dykstra R, Eccles C, Hunter M, Ward R, Callaghan PT. A practical and flexible implementation of 3D MRI in the Earth's magnetic field. J Magn Reson 2006;182:75–83. [PubMed: 16828566]
37. Magin RL, Webb AG, Peck TL. Miniature magnetic resonance machines. IEEE Spectrum 1997:51–61.

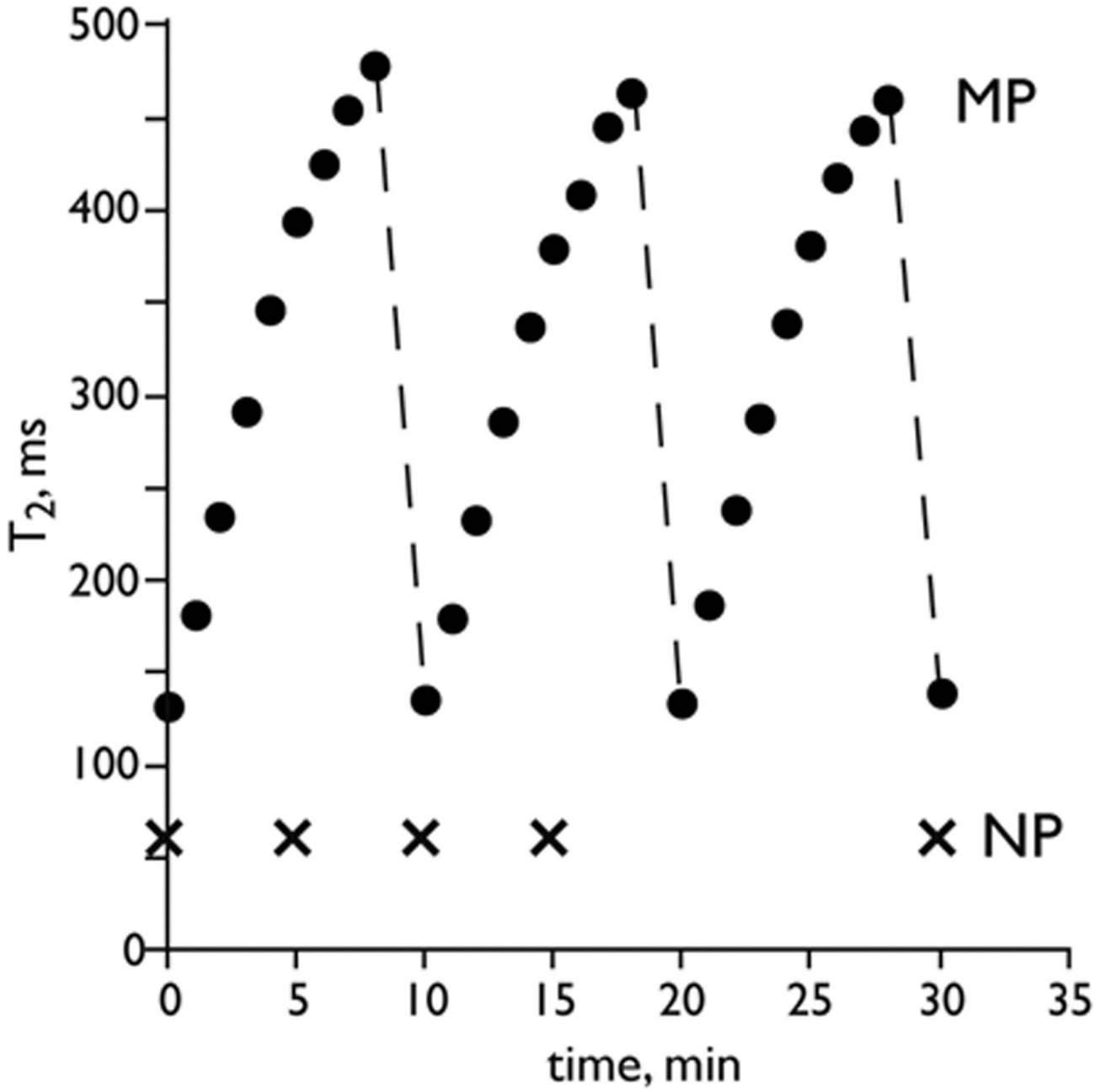

Figure 1.
Time dependence of T_2 with magnetic particles (MP) and magnetic nanoparticles (NP) upon exposure to a homogeneous magnetic field in a relaxometer. T_2 of MP solution increased in the magnetic field (0.47 T) and returned to its original value when removed from the field. T_2 of a NP solution was time independent. Broken line indicated the removal of MP solution from the magnetic field.

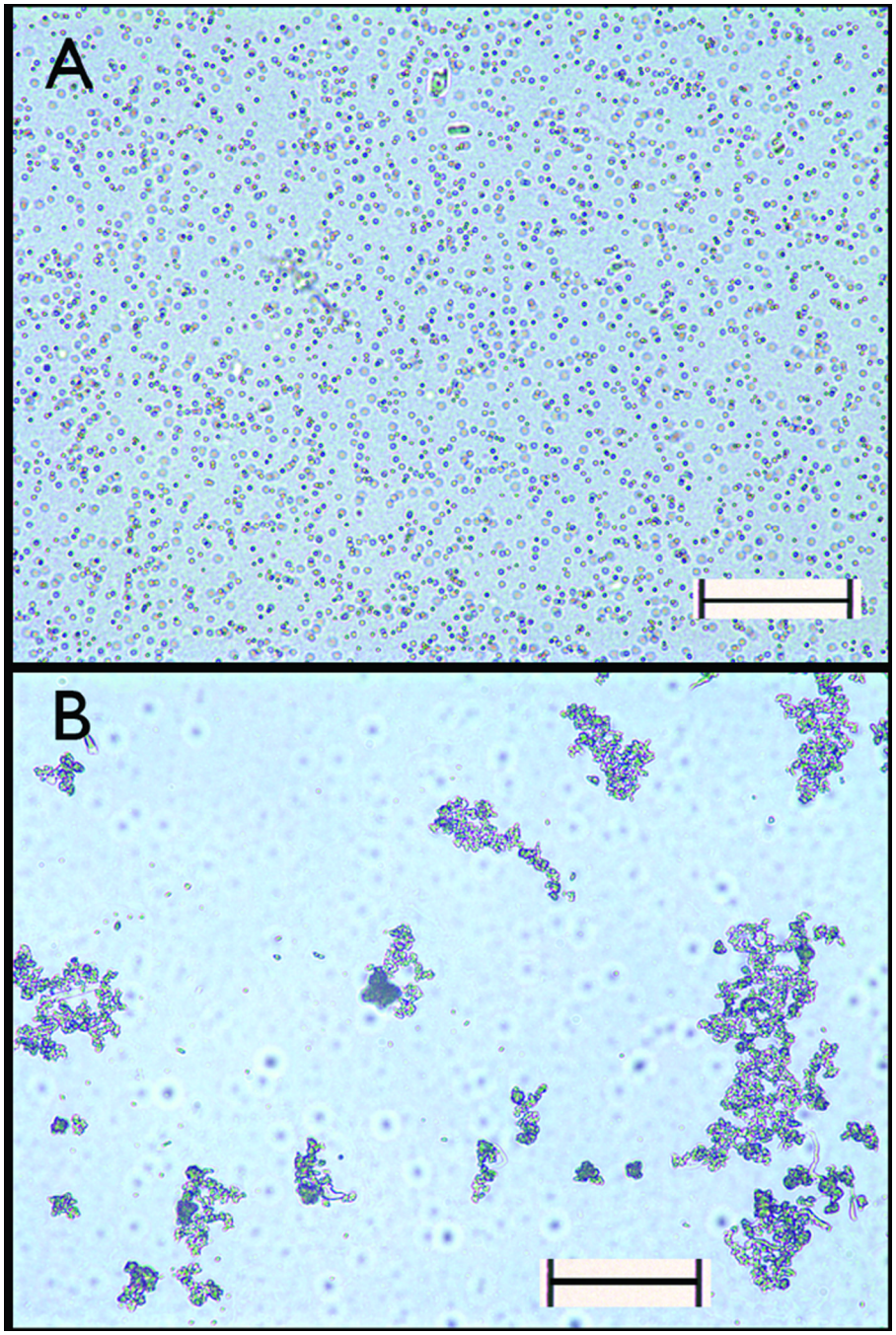

Figure 2.
Magnetic field induced magnetic particle aggregate formation viewed by phase contrast microscopy. (A) Micrograph of dispersed MP immobilized in agar solidified in the absence of a magnetic field. (B) Micrograph of aggregated MPs in agar solidified in a magnetic field of 0.47 T. Scale bars are 50 microns.

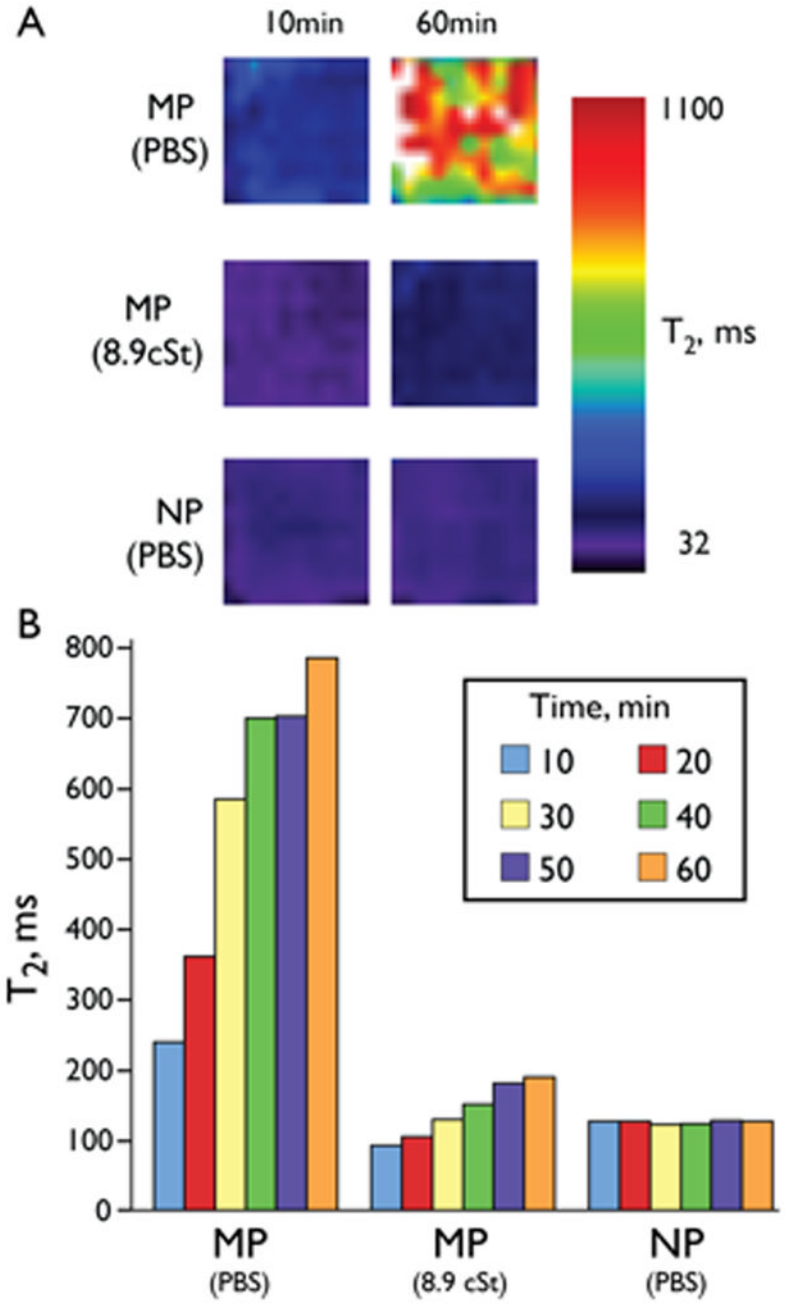

Figure 3.

Magnetic field induced magnetic microparticle aggregation at 4.7 T. (A) T_2 maps of solutions of MPs and NPs at 10 minutes and 60 minutes in a magnetic field (4.7 T, 25 °C). (B) T_2 values of wells shown in (A) at 10-min intervals. A time dependent increase in the T_2 occurred for the MP but not for the NP. With a viscosity of 8.9 cSt, achieved by adding Triton X-100, a smaller increase in T_2 occurred. T_2 values are means for the well.

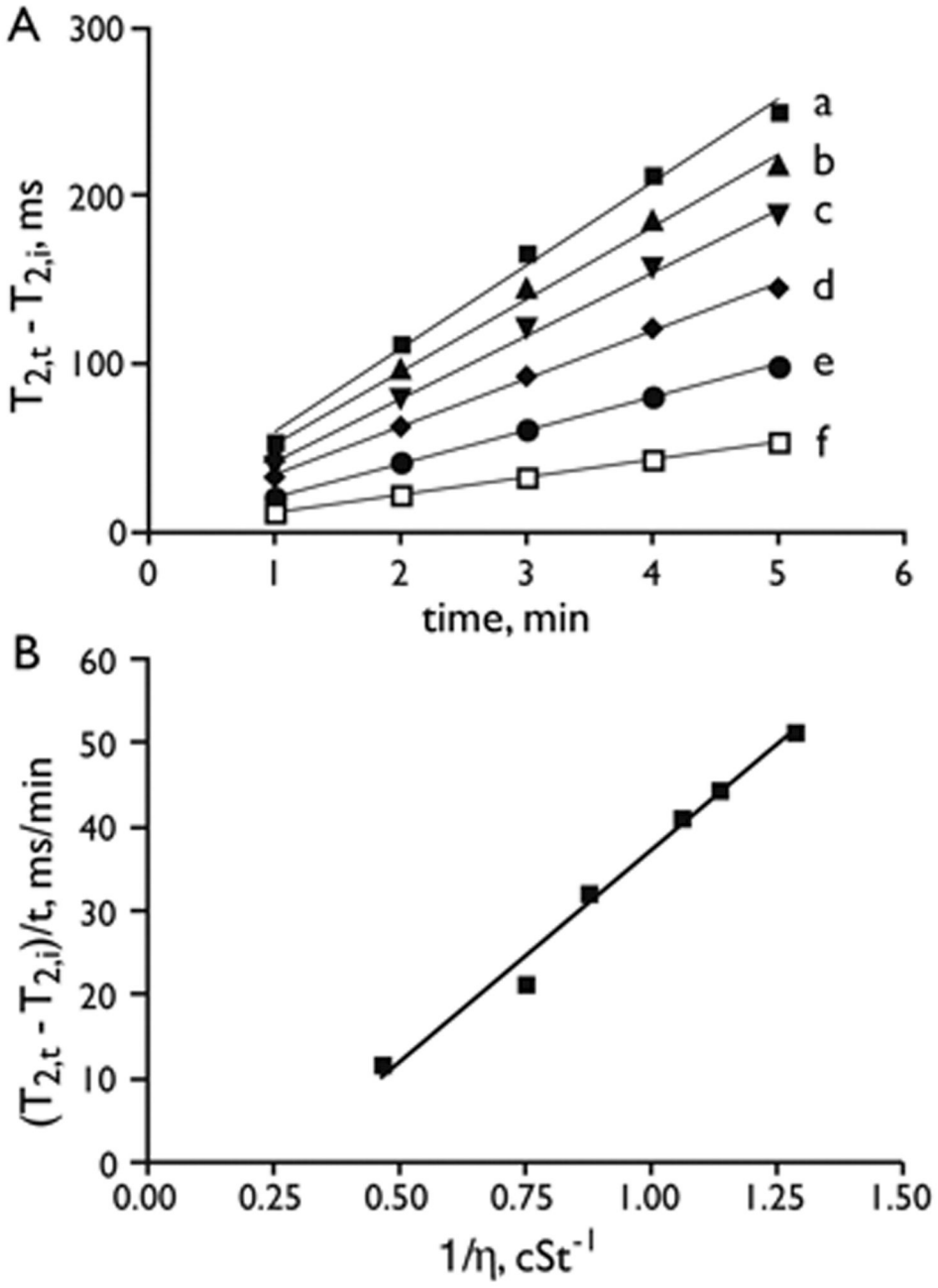

Figure 4.

Viscosity determination of artificial serum using magnetic field induced magnetic microparticle aggregation. (A) Change in T_2 with time for synthetic "myeloma serum" at 0.47 T. $T_{2,i}$ is the initial or starting T_2. $T_{2,t}$ is the T_2 at some time t. The solutions were: a). FBS + 20% PBS (v/v); b). FBS; c). FBS + 10mg/mL bovine IgG (v/w); d. FBS + 20 mg/mL bovine IgG; e). FBS + 50 mg/mL bovine IgG; and f). FBS + 100 mg/mL bovine IgG. (B) The rate of T_2 change from (A) versus the reciprocal of viscosity.

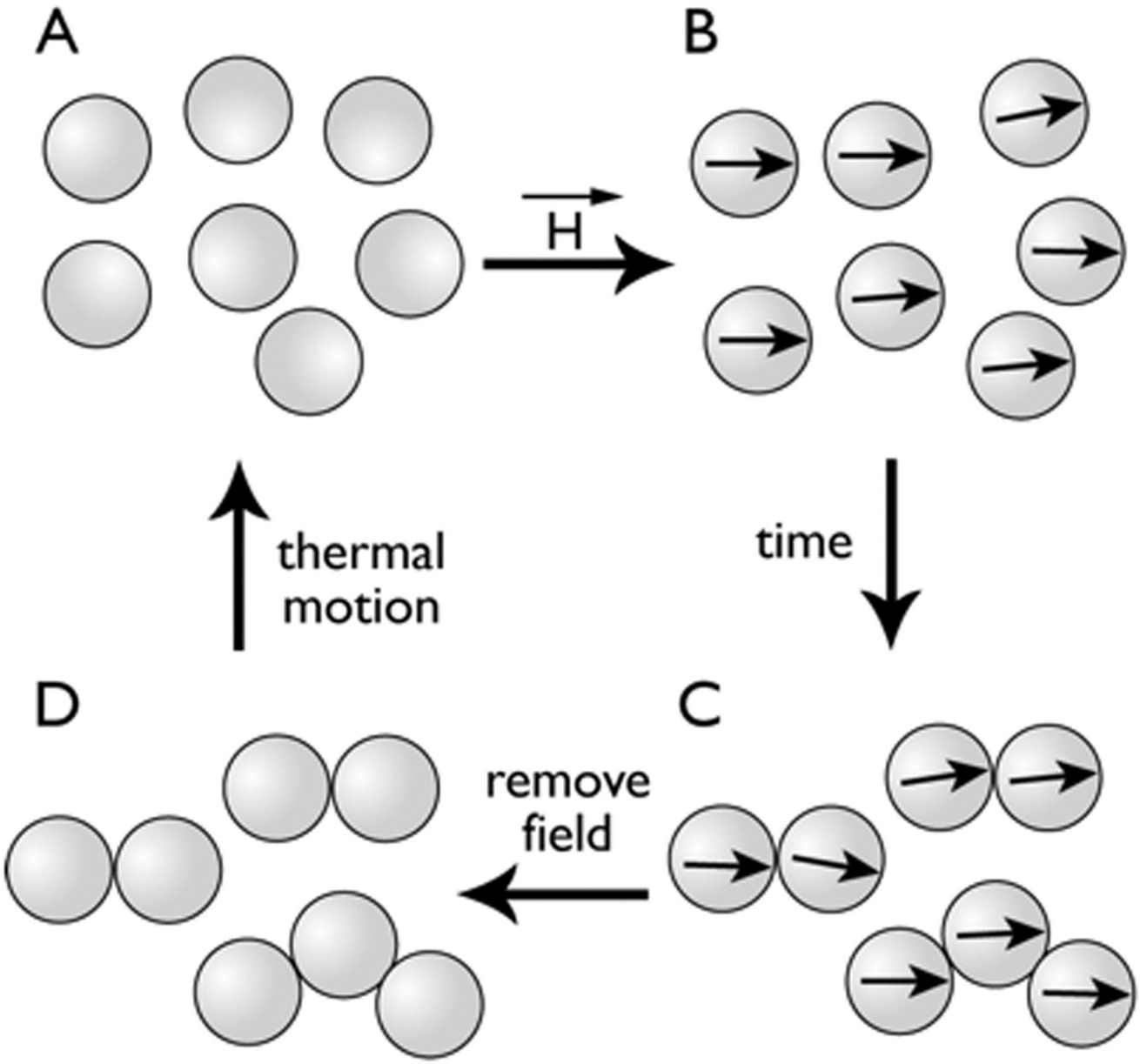

Figure 5.
Reversible magnetic field induced aggregation of MPs. When dispersed MPs (A) are placed in a magnetic field, MPs become magnetic and all magnet moments are aligned with the field (B). Over time, when two MPs come close together, they form aggregates, which are effectively a small number of larger magnets (C). When the field is removed, MPs demagnetize (D). Lacking aligned magnetic moments, MP aggregates return to the dispersed state (A).

Table 1

Physical properties of magnetic microparticles (MPs) and nanoparticles (NPs)

Particle	MP	NP
Size	1000	30
Settling	< 5%	None
R_1/s^{-1} per mM Fe [a]	<1	18
R_2/s^{-1} per mM Fe	43	50
M/emu per g Fe [b]	105	86.6
Fe atoms per particle	2.8×10^9	8, 000
R_2/s^{-1} per mM particle	1.2×10^{11}	400, 000
M/emu per particle	2.6×10^{-11}	6.2×10^{-17}

[a] R_1 and R_2 were measured at 0.47 T, 40 °C

[b] Magnetic moment at 5 T and 25 °C

[c] Relaxivities per particle are the relaxivities per mM Fe multiplied by the number of Fe atoms per MP or NP.